RSC Advances

This is an *Accepted Manuscript*, which has been through the Royal Society of Chemistry peer review process and has been accepted for publication.

Accepted Manuscripts are published online shortly after acceptance, before technical editing, formatting and proof reading. Using this free service, authors can make their results available to the community, in citable form, before we publish the edited article. This *Accepted Manuscript* will be replaced by the edited, formatted and paginated article as soon as this is available.

You can find more information about *Accepted Manuscripts* in the Information for Authors.

Please note that technical editing may introduce minor changes to the text and/or graphics, which may alter content. The journal's standard Terms & Conditions and the Ethical guidelines still apply. In no event shall the Royal Society of Chemistry be held responsible for any errors or omissions in this *Accepted Manuscript* or any consequences arising from the use of any information it contains.

ROYAL SOCIETY OF CHEMISTRY

www.rsc.org/advances

Study of electronic structure, stability and magnetic quenching of $CrGe_n$ (n=1-17) clusters: A density functional investigation

Kapil Dhaka and Debashis Bandyopadhyay
Department of Physics, Birla Institute of Technology and Science, Pilani,
Rajasthan, 333031, INDIA
E-mail: debashis.bandy@gmail.com

Abstract

In the present report the evolution of electronic structure, stability and magnetic quenching of $CrGe_n$ nanoclusters have been carried out using density functional theory (DFT). From the nature of the variation of different thermodynamic and chemical parameters $CrGe_{10}$ and $CrGe_{14}$ ground state clusters are identified as the most stable species. It is observed that the enhanced stability of $CrGe_{10}$ and $CrGe_{14}$ are due to closed shell filled structure of Cr-atomic orbitals and follow 18- electron counting rule. It is found that the strong mixing of Cr d- orbital with the s- and p-atomic orbitals of the Ge atoms in the cluster are mainly responsible for the stability and quenching of Cr magnetic moment in the clusters. Calculated CPs also gives additional information about the bonding and its effect on the stability of the clusters. Calculated IR and Raman spectra are also supports these results.

RSC Advances Accepted Manuscript

1 Introduction

In recent time mid 3d- transition metal encapsulated semiconductor nanoclusters attracted a lot of interest to understand the science behind their electronic structures and stabilities[1-10]. In general, pure silicon and germanium nanoclusters are relatively unstable. However, encapsulation of transition metal atoms in the semiconductor cages can improve the stability of these clusters[11-19]. For appropriate composition and size when the encapsulated clusters have 2, 8, 18, 20, etc. shell closing numbers of valance electrons, the cluster attains an enhanced stability[20–22]. The stability of such clusters sometimes can be explained with the existing theoretical models and sometimes are not. It is worth to mention here that during the hybridization of semiconductor cages with the doped transition metal atoms, the semiconductor atom (Si or Ge) contributes one electron in the cage to make bond with the doped atom[8,9]. On the basis of this hypothesis the transition metal doped semiconductor clusters ($TMSi_n$ or $TMGe_n$) can be taken as 18- or 20- electron (shell closing number) clusters depending upon its size and compositions that gains an enhanced stability. As example, in an ion trap experimental study on cationic MSi_n (M= Hf, Ta, W, Re, Ir, etc.) clusters followed by *ab*-initio calculation Hiura et. al.[23] confirmed the extra stability of WSi_{12} cluster is due to the closed shell electronic (18-electron) structure assuming each Si atom contributing one electron in bonding with W which has 6 valance electrons. Recently, Atobe et al.[24] investigated the electronic properties of transition metal and lanthanide-metal doped anionic Ge_nM (M = Sc, Ti, V, Y, Zr, Nb, Lu, Hf, and Ta) and Sn_nM (M = Sc, Ti, Y. Zr, and Hf) clusters by anion photoelectron spectroscopy and discussed the possibility of transition metal (TM) doped Si and Ge based superatoms which are all 20-electron clusters. A different results on mass spectrographic study of MSi_n (M=Cr, Mo and W) systems were reported by Beck[25,26] where MSi_{15} and MSi_{16} are found as stable products though they are not 18- or 20- electron clusters following the above hypothesis. In a theoretical study, Wang and Han[27] found that $ZnGe_{12}$ is the most stable species in $ZnGe_n$ series, which is not 18-electron cluster. To explain the experimental results of Neukermans[28], Abreu et. al.[1] confirmed that non-magnetic $CrSi_{14}$ cluster is a stable one and it follows 18-electron counting rule by introducing orbital splitting to explain the stability of this cluster. In another theoretical study Guo et al.[13] explained the stability of Si_nM (M=Sc, Ti, V, Cr, Mn, Fe, Co, Ni, Cu, Zn; n=8-16) nanoclusters using shell-filling model where the d-shell of the transition metals plays an important roll in hybridization to form a closed shell structure. The enhanced stability of the transition metal doped Si and Ge clusters were also explained by the considering the formation of a filled shell free-electron gas inside the cage including the geometric effects of the clusters[7]. An extensive theoretical study were reported by Goicoechea and McGrady[29] on

RSC Advances Accepted Manuscript

the stability of $TMSi_{12}$ and $TMGe_{12}$ clusters on the basis of the availability of total number of valance electrons in the ground state of deltahedral or prismatic structures. In these clusters the maximum stability is associated with both doped TM metal atom and cage. When both of them will share the electron density in such a way that both components attain a closed-shell configuration, so that 18- electron counting rule will be followed. In the present work our main focus is to explain the enhance stability of singlet ground state $CrGe_{10}$ and $CrGe_{14}$ nanoclusters and also the quenching of magnetic moment when the clusters evolve from Ge-Cr dimer state due of the hybridization with the cage atoms. Since the properties of these kinds of nanoclusters can be varied in a wide range by changing the doping elements, therefore, these classes of clusters may be valuable for several semiconductor industries. With these fundamental interests in science and technology, we performed a detailed study on the chromium encapsulated germanium system mainly to answer some of the questions related to the stability and quenching of magnetic moments by studying different thermodynamical and chemical parameters, analysis of Cr- atomic orbitals in clusters, hybridization of Cr d- orbitals, critical points (CP's), PDOS, TR and Raman spectra during the growth process of the cluster in the size range from n=1 to 17.

2 Computational

Complete calculations splits into two parts mainly. All geometry optimizations were performed with no symmetry constraints. During optimization, it is always possible that a cluster with particular guess geometry is trapped in a local minimum of the potential energy surface. To avoid this, we used a global structure predictor method using USPEX (Universal Structure Predictor: Evolutionary Xtalloraphy)[30] and VASP (Vienna AB-inition simulation package)[31,32] to get all possible optimized geometric isomers in each size, from n=8 to 17. VASP code has been used to relax the structures predicted by USPEX. For this, we have used combination of few-set of pseudo-potentials available in VASP. In the next stage of optimizations and post optimization calculations, the last few low energy isomers obtained from USPEX and VASP were re-optimized at different spin states in Gaussian' 09[33] to obtain different energy parameters. Here, all calculations were performed within the framework of linear combination of atomic orbital's density functional theory (DFT). The generalized gradient approximation (GGA) calculation were carried out under the exchange-correlation potential as proposed by Perdew, Burke and Ernzerhof commonly known as PBE method[34,35] available in Gaussian '09. Different basis sets were used for germanium and chromium. Full electron 6-311G standard basis set available in Gaussian'09 for Cr and LanL2DZdp with effective core potential (ECP) obtained from EMSL basis set exchange[36] for germanium are used to express molecular-orbitals of all atoms

RSC Advances Accepted Manuscript

as linear combinations of atom-centered basis functions. LanL2DZdp is a double-basis set with a LANL effective core potential (ECP) and with polarization function[37,38]. Unless specified otherwise, the results presented are obtained using the Gaussian'09 program package. Demon2k program package[39] is used to calculate the critical points (CPs) inside the ground state clusters.

3 Result and discussions

3.1 Geometries and thermodynamic parameters

Variations of different thermodynamic and chemical parameters during the growth process are the initial evidences to identify stable nanoclusters. We have studied the growth of the doped clusters within the size range n=1 to 17.

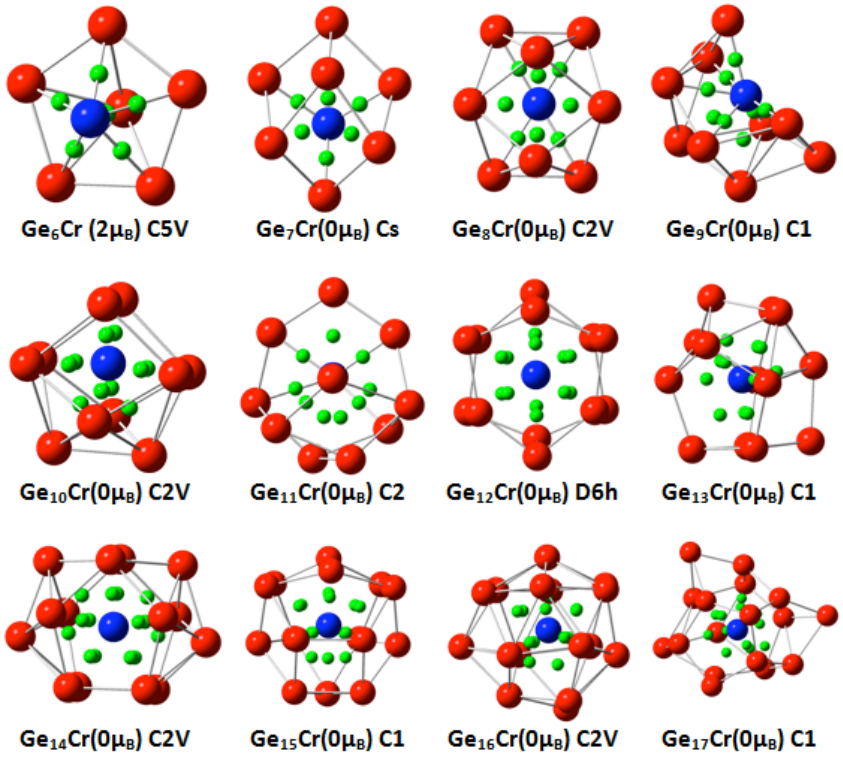

Fig. 1 Ground state geometries and (3,-1) BCPs of $CrGe_n$ (n =6-17). Red, blue and green spheres are denoting 'Ge', 'Cr' atoms and the positions of BCPs belong to Cr atom, respectively.

Optimized ground state structures and corresponding spin magnetic moments along with the calculated bond critical points (BCPs) of $CrGe_n$ clusters are shown in Fig. 1 (Also see Fig. SI1 for other low energy isomers) . More detailed geometries at different sizes is presented in SI, To study thermodynamic stability, we have calculated the variation of average binding energy (BE), embedding energy (EE), fragmentation energy (Δ), stability or the 2nd order change in energy (Δ_2) and ionization potential of the clusters, detachment energies etc. We define the BE, EE, FE, stability, VIP and ADE as follows:

RSC Advances Accepted Manuscript

$$BE = \left(nE_{Ge} + E_{Cr} - E_{Ge_nCr}\right)/\left(n+1\right);\ EE = \left(E_{Ge_n} + E_{Cr} - E_{Ge_nCr}\right)$$
$$FE = \Delta\left(n, n-1\right) = \left(E_{Ge_{n-1}Cr} + E_{Ge} - E_{Ge_nCr}\right)\ Stability = \Delta_2 = \left(E_{Ge_{n+1}Cr} + E_{Ge_{n-1}Cr} - 2E_{Ge_nCr}\right)$$
$$AIP\ or\ VIP = E_{CrGe_n} - E_{CrGe_n^+};\ ADE\ or\ VDE = E_{CrGe_n^-} - E_{CrGe_n}$$

where, M is the total spin of the cluster or the atom in units of ħ. Since the all ground state $CrGe_n$ clusters in the range n=1-6; and n=16 are magnetic, therefore in the present study, the binding energy and embedding energy of these clusters are calculated after imposing Wigner-Witmer spin-conservation rule[40] following our previously reported wotk[7-9]**.** Imposing this rule the modified expressions of BE and EE are defined as follows:

$$BE^{WW} = \left[nE\left({}^0Ge\right) + E\left({}^MCr\right) - E\left({}^MGe_nCr\right)\right]/\left(n+1\right)$$
$$EE^{WW} = E\left({}^MGe_n\right) + E\left({}^0Cr\right) - E\left({}^MGe_nCr\right) or,\ E\left({}^0Ge_n\right) + E\left({}^MCr\right) - E\left({}^MGe_nCr\right)$$

In the above binding energy and embedding energy expressions, we have chosen the higher of the resulting two BE and EEs. In the region for n<7 the binding energy of neutral and cationic clusters increase rapidly. This is an indication of thermodynamic instability of the clusters. For the clusters with size n>7 binding energy increases with relatively slower rate and then reaches nearly a saturation value with small variations. Between n=1 to 6 the ground state clusters are in different spin magnetic states. The clusters show magic nature (stable nature) with localized peaks at n=10 and 14 (Fig 2a). Compare to the binding energy, the magic nature of the clusters are clearer in EE variation. Above n=6 size, a number of local maxima arise at n = 8, 10 and 14 indicate these clusters are more stable compare to its nearby clusters (Fig. 2a). Variation of fragmentation energy (FE) is another important evidence to check the stability of the clusters. Following the expression, FE indicates the gain in energy by a cluster during its growth process by absorbing germanium atoms one by one starting from a Ge-Cr dimer. With reference to the FE variation (Fig 2b), at n = 8, 10 and 14 clusters are more stable compare to its neighboring sizes. The variation of 2nd order change in energy or stability (Δ_2) (Fig 2b) shows magic behavior at n=10 and 14. On the basis of the thermodynamic parameters we found that n=8, 10 and 14 clusters are relatively more stable compare to the other sizes. In the present discussion we are mainly concern about the endohedrally-doped clusters. Though the ground state isomer at n=8 is thermodynamically stable, but the Cr atom absorbed on the surface of the Ge_8 cage to form a hybrid $CrGe_8$ cluster. Since the Cr atom is exposed, the chemical affinity is higher compare to the endohedrally-doped clusters. Therefore, we are not interested on the thermodynamic stability of this cluster.

In order to understand, how the removal or addition of one electron is changing the chemical stability of the clusters, we have calculated ionization potentials (AIP and VIP) and HOMO-LUMO gap (Fig. 2c); and detachment energies

RSC Advances Accepted Manuscript

(VDE and ADE) (Fig. 2d). Variation of AIP and VIP nature are similar with a small difference between these values in a particular size. There is sharp peaks at n=10 and 14 in the variation of ionization potential with a maximum value at n=14 indicated the $CrGe_{14}$ is the most table cluster among all. Variation of HOMO-LUMO gap with the growth of the cluster is one of the important evidence to understand the closed shell nature of the clusters. With reference to the Fig. 2c, both $CrGe_{10}$ and $CrGe_{14}$ have almost equal HOMO-LUMO gap of close to 1.29 eV. There is clear dip in HOMO-LUMO gap variation at n=12 and 16 with values 0.78 eV and 0.57 eV respectively among the endohedrally doped clusters. The cause of the enhance stability of n=10 and 14 clusters will be discussed in the next section on the basis of molecular orbital analysis. We have calculated vertical detachment energy (VDE) and adiabatic detachment energy (ADE) following the equations mentioned in the previous section. Here, VDEs are the energy differences between the anionic and neutral cluster at a particular size keeping the geometry of the cluster unchanged. Whereas, ADE defines the energy difference between the anionic ground state and neutral ground state in a particular size of a cluster. In the later case, geometry of these two clusters may be different. The variation of VDE and ADE with the cluster size shown in Fig. 2d support the results obtained from the AIP, VIP and HOMO-LUMO gap variations of the clusters. The clear local minima at n=10 and 14 indicate that it is easy to remove electron from anionic state in these cluster and hence an indication of the enhance stability of these clusters. With reference to our calculation of thermodynamic and chemical parameters, we found that $CrGe_{10}$ and $CrGe_{14}$ clusters are relatively stable compare to the other clusters in the series.

From our previous discussion, it is clear to take n=10 and 14 clusters can be taken as the stable clusters. We need to make it clear why these clusters are stable and but not n=12. Here we apply molecular and atomic orbital analysis to explain it. First we will discuss the cause of lower stability of $CrGe_{12}$ ground state cluster. The $CrGe_{12}$ ground state cluster is a well-known hexagonal prism with D_{6h} symmetry with an endohedrally doped Cr atom between two hexagonal rings of Ge atoms with 54 valance electrons (6 from Cr: $3d^5$ $4s^1$ and 4 from each Ge: $3s^2$ $3p^2$) in singlet spin state. With reference to the Fig. 3, the orbital energy levels are assigned based on orbital composition. There are total 27 filled energy levels with paired electrons indicating quenching of the Cr spin moment (See Fig. SI2 for details orbital pictures). The electronic distributions can be written in the following sequence: $1S^2$, $1P^6$, $1D^8$, $1F^8$, $2S^2$, $1D^2$, $1G^2$, $1F^4$, $1G^2$, $2P^4$, $2D^8$, $2P^2$, $2D^4$ (HOMO) and $2D^2$ (LUMO). Here we assign the orbitals following method adopted by Abreu et al[1] and we also found that jellium model[41] is incompatible to explain the electronic structure of this cluster because of the presence of 12 electrons in 2D orbital. One of the 2D orbital ($2D_z^2$) appears in

RSC Advances Accepted Manuscript

LUMO. This could be due to the crystal-field like splitting[42] in molecular orbital in the cluster. To understand whether 18- electron rule can be applied or not, we have analyzed one-electron orbitals of Cr in $CrGe_{12}$ cluster. With reference to the recent report by Goicoechea and McGrady[29] since Cr is in the 6th column in the periodic table, therefore, one of its 3d level will pushed up to higher side of the energy level in $CrGe_{12}$. To find out the contribution from Cr in the MOs we have used a fragment analysis where clusters are divided into Cr and Ge_{12} fragments[35,43]. Using this analysis we found reasonable amount of contribution from Cr- $3d_z^2$ atomic orbital in LUMO which being pushed up from the lower level. This also could be the reason of good amount of HOMO-LUMO gap of 0.82 eV in this cluster. The result of one-electron orbitals is shown in the Fig. 3. Since the LUMO contains the $3d_z^2$ orbital contribution of Cr, which is unfilled, therefore, total number of electrons occupied these orbitals are 16 (Fig. 3). Since one 3d orbital (LUMO: $3d_z^2$) is unfilled, therefore, 18- electron rule cannot be applied here. This could be the possible reason why $CrGe_{12}$ does not show stable nature in the thermodynamic and other parameter variation (Fig. 2). In this context, we can recall our discussion in earlier section of this work where we discussed the results of Hura et al.[23] the WSi_{12} cluster can be taken also as 16- electron cluster. Compare to $CrGe_{12}$, both $CrGe_{10}$ and $CrGe_{14}$ have higher values of BEs, EEs, FEs, Δ_2s, IPs and HOMO-LUMO gaps. Applying the same method on $CrGe_{10}$ and $CrGe_{14}$ clusters, we found both of them follow 18- electron rule. In case of $CrGe_{10}$, assigned molecular orbitals may not follow a particular structure, but signature of contribution from Cr in these orbitals is clearly seen. The signature supports Cr contribution results in our calculations. On the basis of that, we have assigned the Cr- atomic orbitals are filled with a configuration $4s^2$, $4p^6$ and $3d^{10}$ (Fig. 4). Hence all atomic orbitals of Cr- are engaged. In this case the Cr metal atom and the cage shared the electron density in such a way that both of them fulfill 18- electron counting. The same is true in the electronic structure of $CrGe_{14}$. In fact, Cr- contributions are clearer in $CrGe_{14}$ cluster. Due to the hybridization between Cr- d orbital with caged Ge- 4p orbital, producing two Cr- $3d_{xz}$, one Cr- $3d_{yz}$ and one Cr- $3d_{yz}$+$4p_z$ mixed orbitals (Fig. 5). In $CrGe_{14}$ LUMO is assigned as $3d_{xy}$. Therefore, $CrGe_{10}$ and $CrGe_{14}$ follow 18- electron counting rule, but it cannot be applied in $CrGe_{12}$ as per out results.

RSC Advances Accepted Manuscript

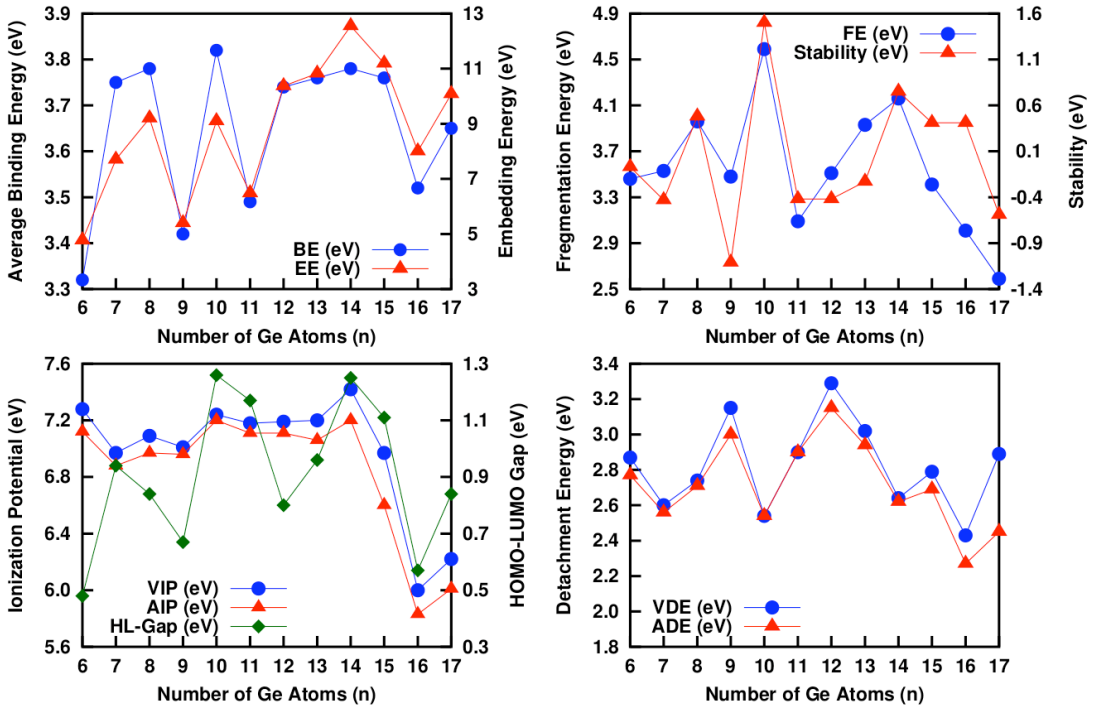

Fig. 2 Variation of average binding energy, embedding energy, fragmentation energy, stability, VIP,AIP, HL-Gap, VDE and ADE of the clusters during growth process.

To investigate the strength of Ge-Ge and Ge-Cr interaction with the increasing size of the clusters, and also to understand the bonding nature, we have calculated the number of different bonds present in the clusters. We have calculated the bond critical points (BCPs) and cage critical points (CCPs) (See Fig. SI3 for RCPs and CCPs) and their locations in the cage to interpret the nature of bonding present in the cage based on the work reported by Bader[44]. The chemical interaction between the fragments of a given sets of molecules can be characterized by the Laplacian of electronic densities. When the density is positive it describes the closed shell bonding, and when it is negative, it is covalent bonding. The critical point is one where this electron density vanishes in 3-D. Therefore this is a position on the bond and reflecting the existence of presence of a bond. A particular CP is characterized by (R,S) where R is the rank of the Hessian matrix of the electron density reflecting the number of Eigen values of the matrix and S is sign of the sum of the Eigen values (either, maxima or minima or saddle) indicating the topological feature. A bond critical point (BCP) in general represented by (3,-1) CP reflecting the saddle point between two molecules or cluster form bonds between them. With this background, we have calculated the BCPs and is shown in Fig. 1. First we have calculated the location of (3,-1) CP's. It is clearly seen that in all endohedrally doped clusters, a number of (3, -1) CP's inside the cages almost uniformly distributed surrounding the encapsulated Cr atom and the number

RSC Advances Accepted Manuscript

varies from cluster to cluster. The ten (3,-1) CPs are indicating the existence of ten bonds between the Cr and germanium atoms in $CrGe_{10}$. The number of Ge-Ge bonds for the clusters in the size rang n=6-12 varies between 16-18, and then it starts increasing with a maximum value of 39 at n=16. Among several isomers (ten) in $CrGe_{16}$, the ground state structure is well known Frank-Kasper polyhedron,[12] which is stable in general. For the cluster with n=6 to 15, Cr is attached with all Ge atoms in the cage and hence the number of bond critical points (BCPs) are same as the number of Ge atoms in the cage. Whereas, due to the higher size of the Ge_{16} and Ge_{17} cage, the Cr atom won't be able to form bonds with a number of Ge atoms in the cage and hence the number of BCPs drops. This could be taken as the structural phase change from the bonding point of view. Following variation of BCPs with the cluster size (Fig. 6), it increases linearly from n=8 to 14. The maximum value of BCP (3,-1) at n=14 is an indication of strong structural stability with C_{2V} symmetry. Though there is no local maxima in BCPs variation at n=10, but there is a clear increasing trend. The maximum value of Ge-Ge bond at n=16 is the indication of stable nature of pure Ge_{16} cage. There is also a local peak at n=10 in the number of Ge-Ge bond variation. Therefore, variation of BCPs and also the number of Ge-Ge bonds in the germanium cages help to understand the stability of the clusters from the structural point of view[45].

RSC Advances Accepted Manuscript

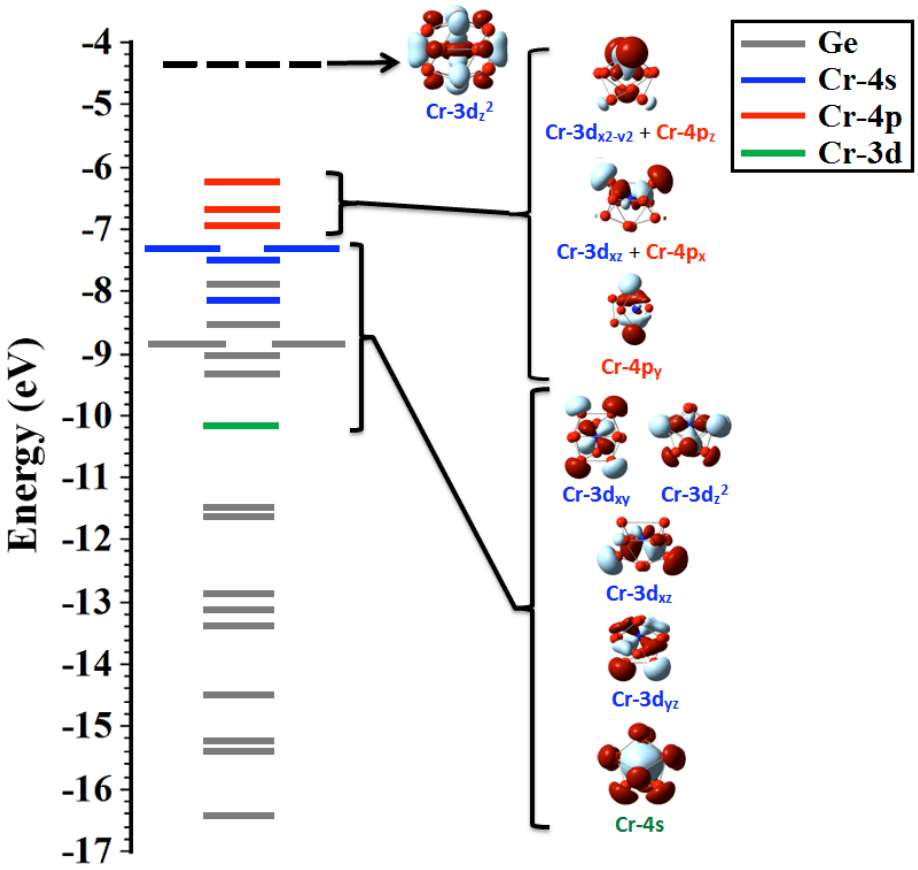

Fig. 3 Molecular Orbitals (MO's) of $CrGe_{10}$ (with Cr contribution).

RSC Advances Accepted Manuscript

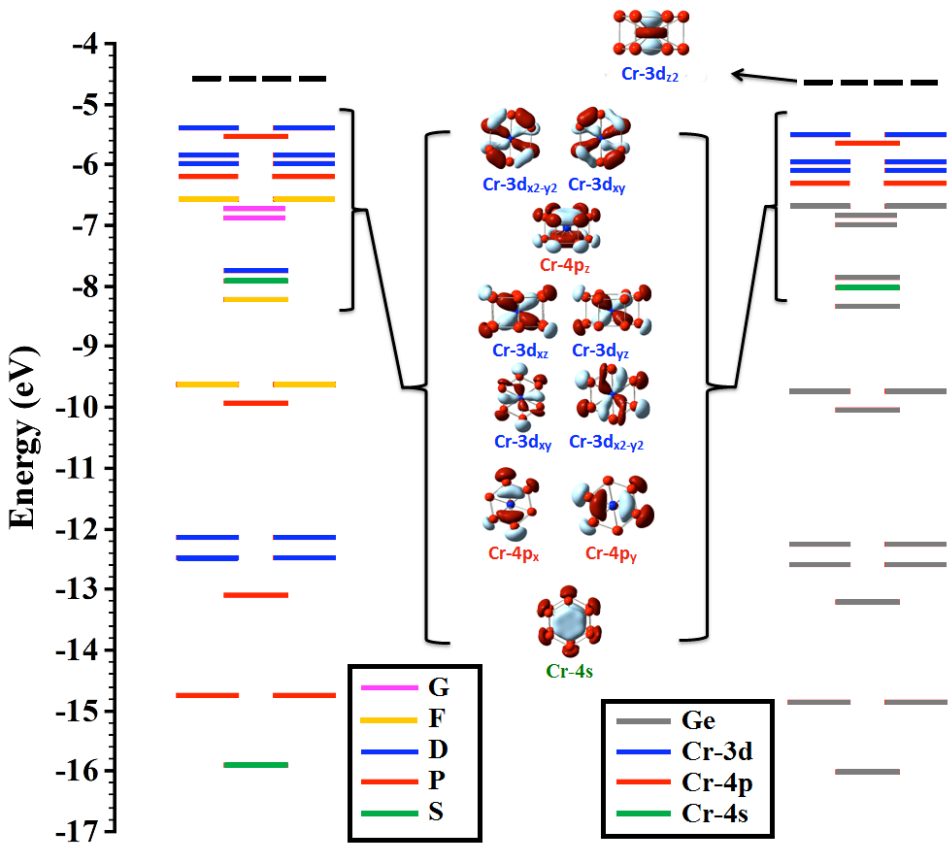

Fig. 4 Molecular Orbitals (MO's) of $CrGe_{12}$ (with Cr contribution).

RSC Advances Accepted Manuscript

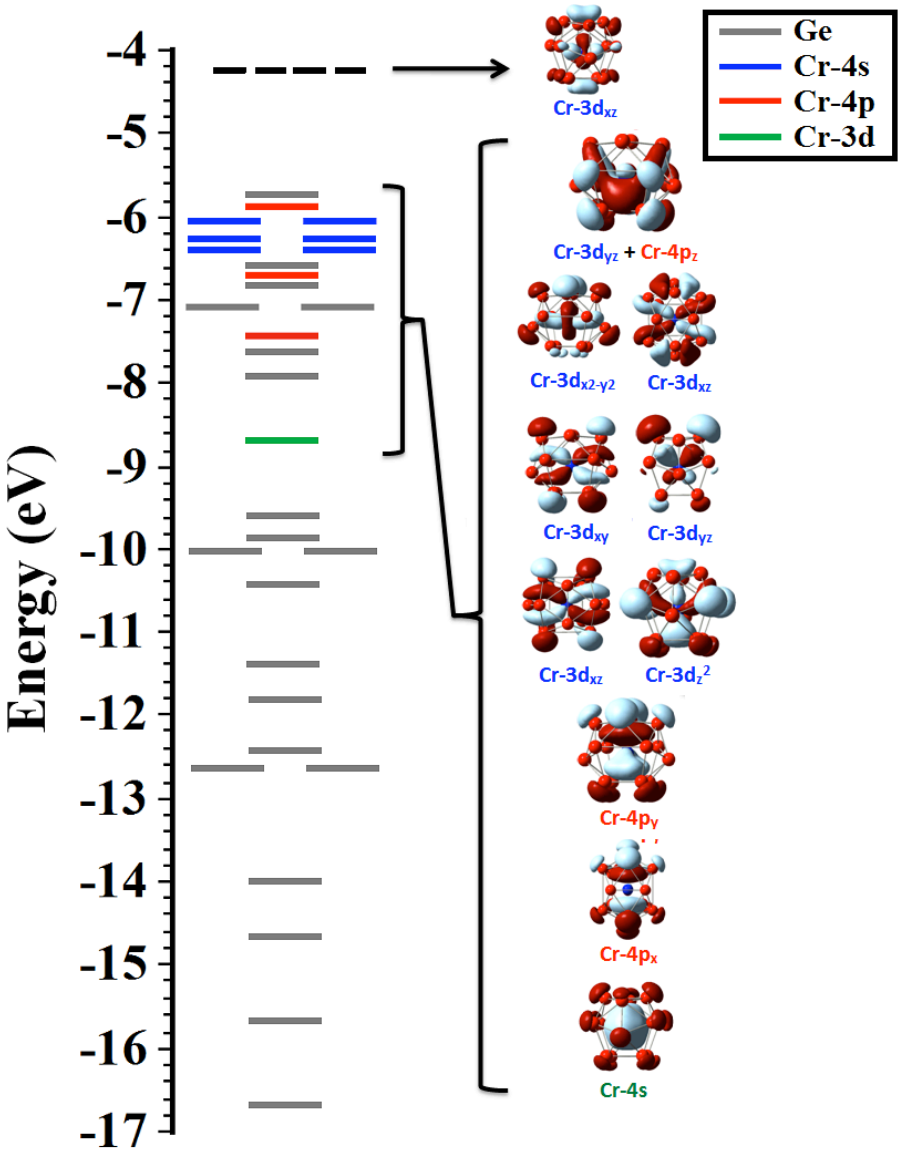

Fig. 5 Molecular Orbitals (MO's) of $CrGe_{14}$ with Cr contribution.

RSC Advances Accepted Manuscript

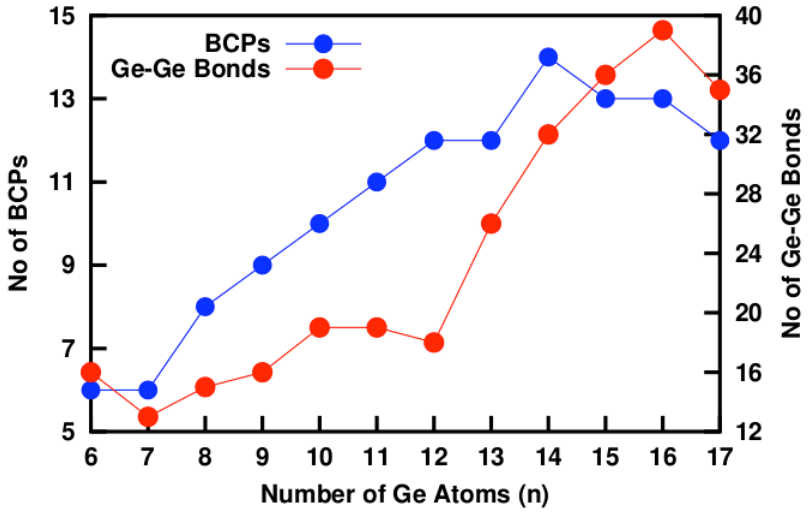

Fig. 6 Bond critical points (BCPs) and No of Ge-Ge bonds.

With the reference to IR and Raman frequencies (Fig. 7) of the clusters from n=6 to 17, at =10, 14 and 16, the number of dominating frequencies are much lesser than the other structures. Less number of modes in IR is basically the indication of the vibration of the bonds (stretching) present in the structure at almost constant frequency or within very small frequency range. This is because of the strong structural symmetry for n=10, 14 and 16. Raman frequency in general indicates the bending mode in the clusters. The narrow peak at n=10,11 and 16 in Raman spectrum indicating the less number of bending modes present in these clusters with a breathing mode (where all the molecules in cage vibrate in phase) with a maximum intensity at 210, 201 and 170 cm^{-1} respectively.

RSC Advances Accepted Manuscript

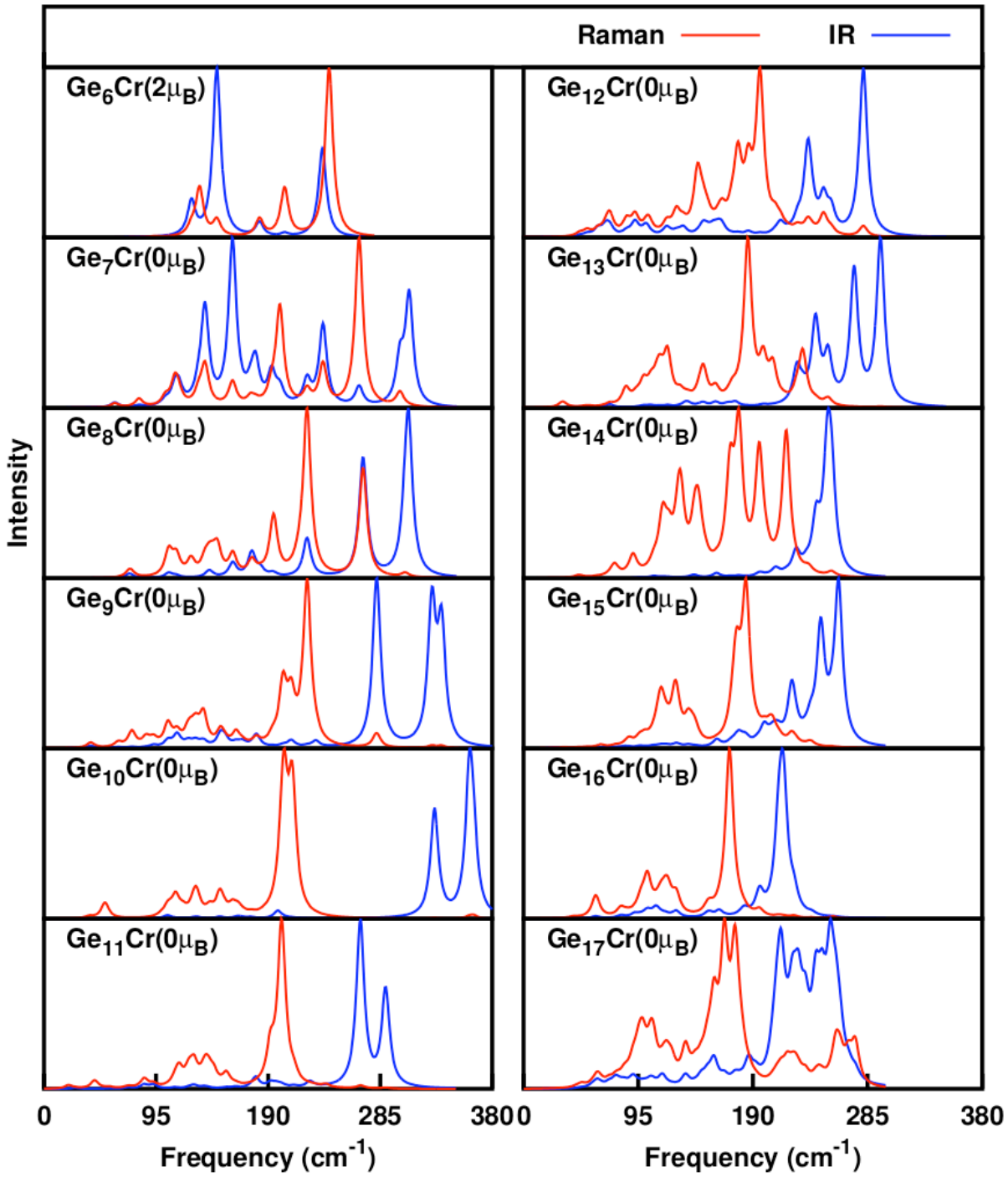

Fig. 7 Variation of IR and Raman spectrum. The intensity is plotted in arbitrary unit.

To understand the strength of Ge and Cr- d orbital contributions in hybridization and the cause of magnetic moment quenching of Cr in the clusters, we have studied PDOS (Fig. 8 and SI); and the percentage of Cr d- alpha and beta

RSC Advances Accepted Manuscript

orbital contribution in hybridization shown in Fig. 9. Since n=1-6 are in quintet or in triplet spin states, therefore, there PDOS is asymmetrical (Fig. 8a and Fig. SI4). For other clusters, in singlet spin states, both alpha and beta contributions in PDOS are identical. In all the stable clusters, there is no contribution of DOS on Fermi level and the HOMO-LUMO orbitals are also clearly separated. The percentage contribution of Cr d- orbital in hybridization is also supports the DOS nature. For n=6, the percentage contributions in hybridization of Cr -d alpha and beta are not same. Therefore, it is clear that the existence of the magnetic moment due to the unequal alpha and beta Cr -d orbital contribution in the hybridization is the main cause of the magnetic moment. With the increase of the size of the clusters from n=1 by adding one by one Ge atoms, the chances of hybridization between the Cr with the Ge atoms increases. Due to this hybridization Cr d- orbital, which is responsible for magnetic moment of Cr decrease and hence the magnetic moment of Cr quenches. So the existence of magnetic moment or the quenching

RSC Advances Accepted Manuscript

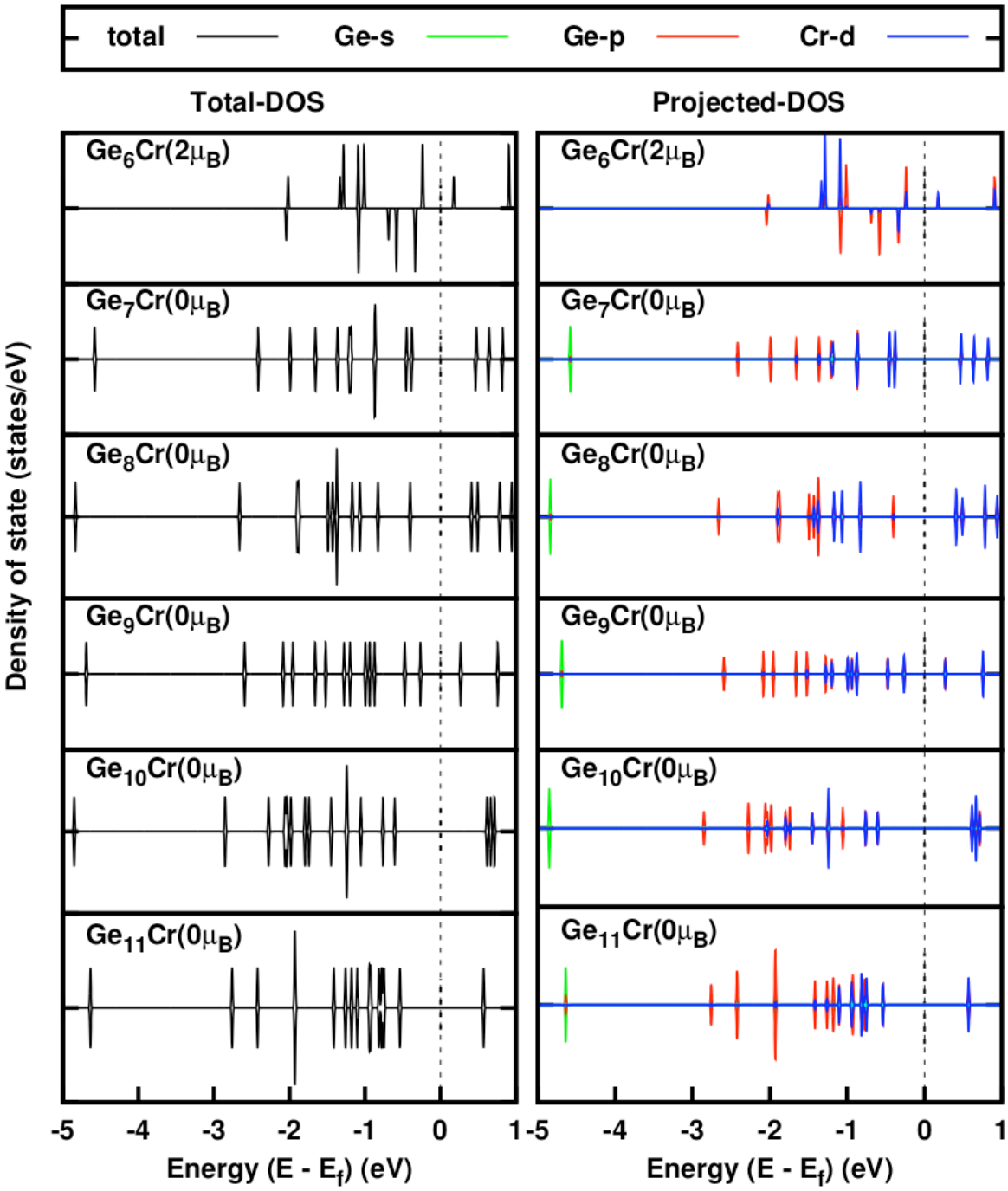

Fig. 8a Variation of DOS and PDOS of different neutral clusters $CrGe_n$ (n=6-11) with shifted energy ($E-E_F$) and Fermi energy is set to '0'

of the magnetic moment of $CrGe_n$ is due to the hybridization between the Ge p- and Cr d- orbital contribution. In case of n=16, the number of Ge-Ge bonds are maximum in the whole series of study (Fig. 6). This is the indication of stable nature of Ge_{16} germanium cage.

RSC Advances Accepted Manuscript

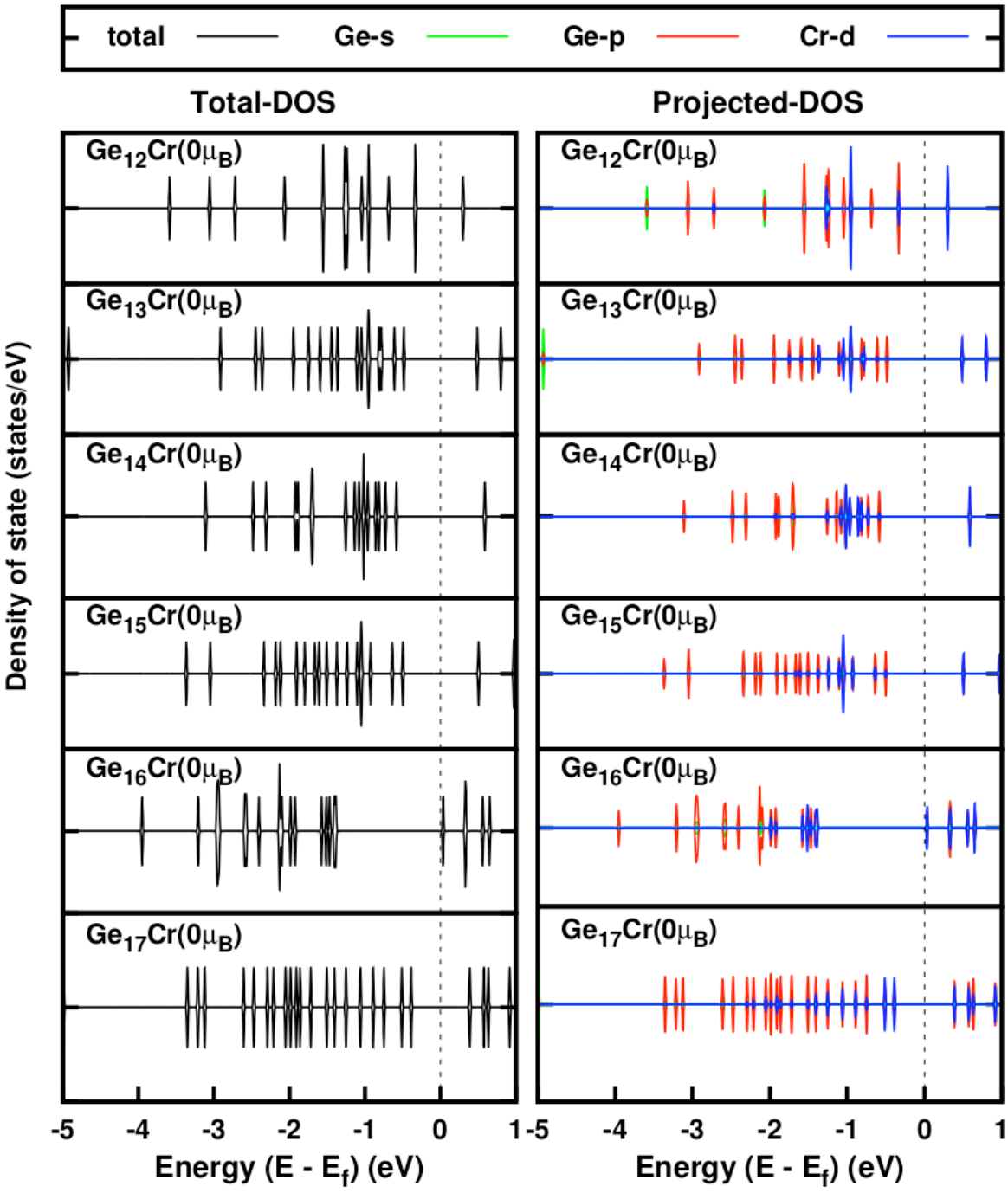

Fig. 8b Variation of DOS and PDOS of different neutral clusters $CrGe_n$ (n=12-17) with shifted energy ($E-E_F$) and Fermi energy is set to '0'

In the clusters, the magnetic moment or the quenching of the magnetic moment is due to the hybridization between the Ge p- and Cr d- orbital contribution. In all the stable clusters, there is no contribution of DOS on Fermi level and the HOMO-LUMO orbitals are also clearly separated.

RSC Advances Accepted Manuscript

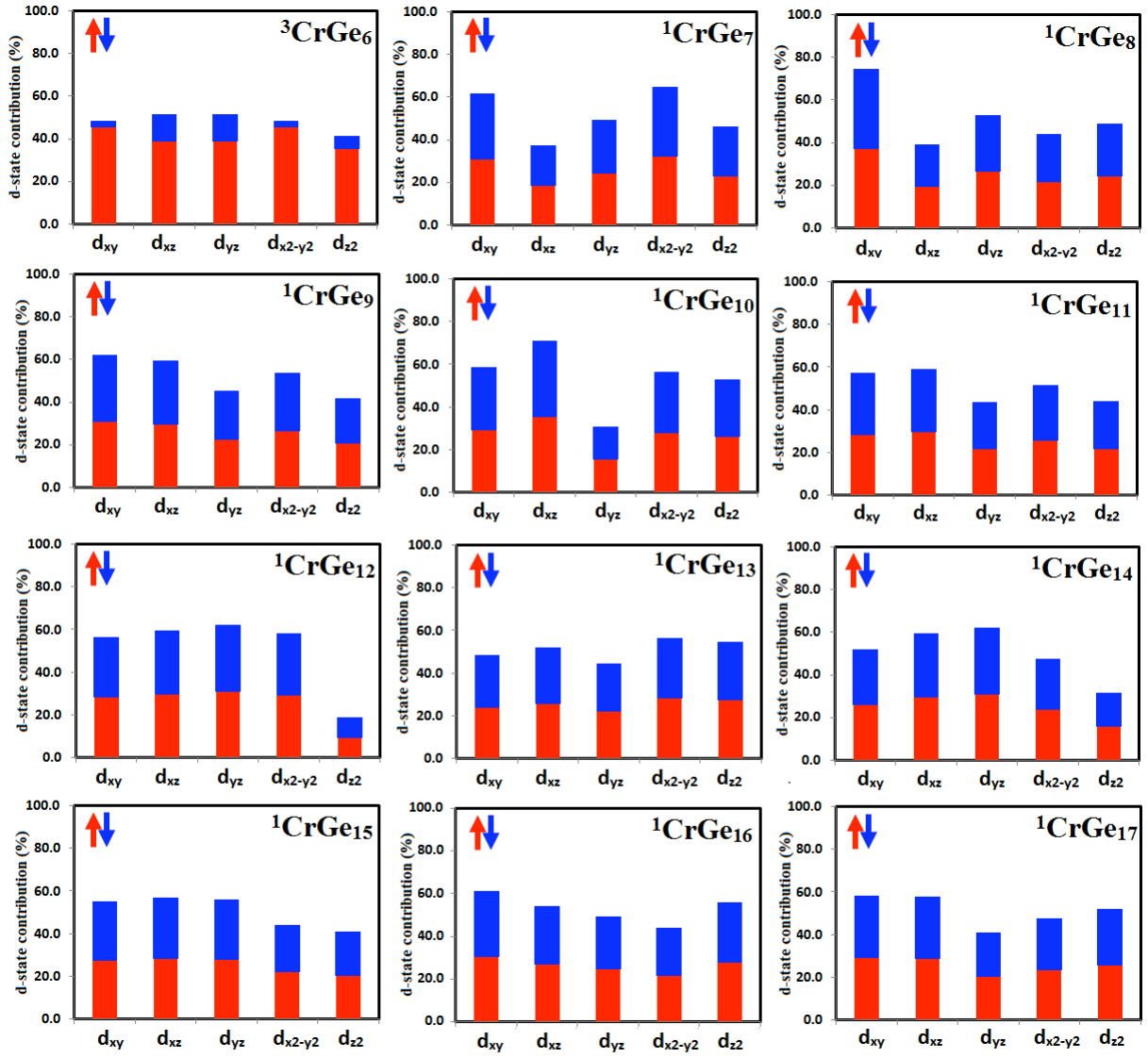

Fig. 9 Percentage of alpha and beta Cr d- orbital contributions in hybridization with Ge_n (n=6-17) cages.

4 Conclusions

The variation of different energy parameters as BE, EE, FE, stability, HOMO-LUMO gap, VIP, AIP, ADE and VDE of the clusters support the enhanced stability at n=10 and 14. The above results point to a more unified picture for the stability of $CrGe_n$ clusters. We have verified electron-counting rule on the basis of Cr atomic filled shell in molecular orbitals. Analysis of Cr atomic shell contributions in molecular orbitals are explained the stable nature of $CrGe_{10}$ and $CrGe_{14}$ clusters. However, $CrGe_{12}$ is less stable due to 16 electrons in Cr shell with electronic configuration of $4s^2$, $4p^6$, $3d^8$. In $CrGe_{12}$ cluster, due to crystal field like splitting Cr- $3d_z^2$ pushed up to LUMO. However, $CrGe_{10}$ and $CrGe_{14}$ are both have Cr atom with electronic configuration of $4s^2$, $4p^6$, $3d^{10}$ which is close

RSC Advances Accepted Manuscript

filled configuration and follow 18 electron counting rule. The analysis of the bond critical points indicates that the more stable species have higher number of BCPs, which leads to an increase in germanium binding energy. The other significant effect, however, is the mixing between the Cr 3d- and Ge p-states which reflected in the PDOS and quenching of the Cr magnetic moments in the clusters. Bonding nature and the vibrational modes present in the clusters can be further understood by the study of the IR and Raman frequencies as discussed. Less number of modes in IR and Raman spectra is basically indicating the higher symmetry in the clusters.

Acknowledgement

A part of the calculation is done at the cluster computing facility, Harish-Chandra Research Institute, Allahabad, UP, India (http://www.hri.res.in/cluster/).

Supporting Information Available

Electronic supplementary information includes Optimized isomers, PDOS of the clusters with the size n=1-5, MOs of n=10, 12 and 14, CCPs and RCPs.

RSC Advances Accepted Manuscript

References

(1) M. B. Abreu, A. C. Reber, S. N. Khanna, J. *Phys. Chem. Lett.* 2014, **5**, 3492–3496

(2) S. N. Khanna, B. Rao, P. Jena *Phys. Rev. Lett*. 2002, **89**, 016803

(3) R. Robles, S. N. Khanna *J. Chem. Phys.* 2009, **130**, 164313

(4) R. Robles, S. N. Khanna Jr, A. Castleman *Phys. Rev. B* 2008, **77**, 235441

(5) R. Robles, S. N. Khanna *Phys. Rev. B* 2005, **72**, 165413

(6) R. Robles, S. N. Khanna *Phys. Rev. B* 2006, **74**, 035435

(7) D. Bandyopadhyay, P. Kaur, P. Sen, *J. Phys. Chem. A* 2010, **114**, 12986–12991

(8) R. Trivedi, K. Dhaka, D. Bandyopadhyay, *RSC Advances* 2014, **4**, 64825–64834

(9) D. Bandyopadhyay, P. Sen, *J. Phys. Chem. A* 2010, **114**, 1835–1842

(10) K. Dhaka, R. Trivedi, D. Bandyopadhyay, *AIP Conference Series* 2013; 1498–1500

(11) D. Bandyopadhyay, *Journal of Applied Physics* 2008, **104**, 084308–084308

(12) V. Kumar, Y. Kawazoe, *Phys. Rev. B* 2002, **65**, 073404

(13) L.-j. Guo, G.-f. Zhao, Y.-z. Gu, X. Liu, Z. Zeng, *Phys. Rev. B* 2008, **77**, 195417

(14) Q. Sun, Q. Wang, T. Briere, V. Kumar, Y. Kawazoe, P. Jena *Phys. Rev. B* 2002, **65**, 235417

(15) V. Kumar, Y. Kawazoe, *Phys. Rev. Lett.* 2002, **88**, 235504

(16) H. Kawamura, V. Kumar, Y. Kawazoe *Phys. Rev. B* 2004, **70**, 245433

(17) H. Kawamura, V. Kumar, Y. Kawazoe, *Phys. Rev. B* 2005, **71**, 075423

(18) K. Dhaka, R. Trivedi, D. Bandyopadhyay *J. Mol. Model.* 2013, **19**, 1473–1488

(19) D. Bandyopadhyay *J. Mol. Model.* 2012, **18**, 3887–3902

(20) J. U. Reveles, P. A. Clayborne, A. C. Reber, S. N. Khanna, K. Pradhan, P. Sen, M. R. Pederson *Nat. Chem.* 2009, **1**, 310–315

(21) W. A. de Heer, Rev. Mod. Phys. 1993, **65**, 611

(22) M. Zhang, J. Zhang, X. Feng, H. Zhang, L. Zhao, Y. Luo, W. *J.* Cao, *Phys. Chem. A* 2013, **117**, 13025–13036

(23) H. Hiura, T.Miyazaki, T.Kanayama *Phys. Rev. Lett.* 2001, **86**, 1733

(24) J. Atobe, K.Koyasu, S.Furuse, A Nakajima,. *Phy. Chem. Chem. Phy.* 2012, **14**, 9403–9410

(25) S. M. Beck *J. Chem. Phys.* 1987, **87**, 4233–4234

(26) S. M. Beck, *J. Chem. Phys.* 1989, **90**, 6306–6312

RSC Advances Accepted Manuscript

(27) J.Wang, J.-G Han *Chem. Phy.* 2007, **342**, 253–259

(28) S. Neukermans, X. Wang *Int. J. Mass Spec.* 2006, **252**, 145–150

(29) J .M. Goicoechea, J. E. McGrady, Dalton Trans., 2015, **44**, 6155

(30) A. R.; Oganov, , C. W. Glass*J. Chem. Phys.* 2006, **124**, 244704

(31) G. Kresse, J.Furthmüller,. *Phys. Rev. B* 1996, **54**, 11169

(32) G.; Kresse, D. Joubert, *Phys. Rev. B* 1999, **59**, 1758

(33) A. Frisch, Gaussian **09**: User's Reference; Gaussian, 2009

(34) J. P. Perdew, K. Burke, M. Ernzerhof, *Phys. Rev.Lett.* 1996, **77**, 3865

(35) J. P. Perdew, K. Burke, M. Ernzerhof, *Phys. Rev.Lett.* 1997, **78**, 1396

(36) K. L. Schuchardt, B. T. Didier, T. Elsethagen, L. Sun, V. Gurumoorthi, , J. Chase, J. Li, T. L. Windus, *J. chem. info. mod.* 2007, **47**, 1045–1052

(37) P. J. Hay, W. R. Wadt, *J. Chem. Phys.* 1985, **82**, 270–283

(38) W. R. Wadt, P. J. Hay, *J. Chem. Phys.* 1985, **82**, 284–298

(39) A. M. Koster, et al. (2006) deMon2k, V. 2.3.6. (The deMon Developers Community, Cinvestav, Mexico),

(40) E. Wigner, E. Witmer, *Z. Phys* 1928, **51**, 859–886

(41) W. Ekardt, *Phys. Rev. B* 1984, **29**, 1558-1564

(42) P.J. Roach, W.H. Woodward, A.C. Reber, S.N. Khanna, A.W. Castleman, Phys. Rev. B 2010, **81**, 195404

(43) W.H. Woodward, A.C. Reber, J.C. Smith, S.N. Khanna, A.W. Castleman, J. Phys. Chem. C 2013, **117**, 7445−7450

(44) R. F. W. Bader, Atoms in Molecules: A Quantum theory (Clarendon Press, Oxford, 1990)

(45) V. Chauhan, M. B. Abreu, A. C. Reber, and S. N. Khanna, Phys. Chem. Chem,. Phys. 2015, **17**, 15718-15724

RSC Advances Accepted Manuscript